TECHNICAL ARTICLE

Experimental Approach to Compare Noise Floors of Various Torsional Vibration Sensors

S. Seidlitz[1], R.J. Kuether[2], and M.S. Allen[2]

1 Cummins Power Generation, Minneapolis, MN, 55432,
2 Department of Engineering Physics, University of Wisconsin-Madison, Madison, WI, 53706,

Keywords
Torsional Vibrations, Rotating Machinery, Noise Floor Measurements, Torsional Laser Vibrometer, Optical Encoder, Angular Accelerometer, Variable Reluctance Sensor

Correspondence
R.J. Kuether,
Department of Engineering Physics,
University of Wisconsin-Madison,
534 Engineering Research Building,
1500 Engineering Drive,
Madison, WI 53706
Email: rkuether@wisc.edu

Received: January 18, 2013;
accepted: May 12, 2014

doi:10.1007/s40799-016-0073-1

Abstract

Various sensors exist for measuring torsional vibrations in rotating machinery. When acquiring torsional vibration measurements on a physical system, it is important that the noise floor of the measurement system be lower than that of the response. The goal of this work is to develop an experiment to compare the noise floor of various torsional vibration sensors. A test fixture has been designed and manufactured in order to minimize the angular acceleration of a rotating shaft, so that it runs at a nearly constant angular velocity. The shaft is equipped with a massive flywheel and a soft drive belt in order to isolate any torque fluctuations from the drive motor. Since the test fixture ideally has minimal angular acceleration, the measurements obtained from the sensors during steady-state rotation should be an estimate of the noise floor of each sensor. Rotational measurements at 1200 rpm are obtained from a range of sensors and compared. The sensors include torsional accelerometers, a rotational laser vibrometer, optical encoders of various sizes, a gear tooth sensor, and an optical sensor on zebra tape. The results show that some sensors have lower noise floors than others, depending on the frequency range of interest.

Introduction

Torsional vibrations frequently lead to failures in rotating machinery including internal combustion engines, electric generators, and transmissions. Torsional vibration measurements have been used for over 100 years to validate design models, diagnose failure, and check that operating vibration levels are not excessive. This is critical for many types of rotating machinery since there are several physics that can cause significant forces at the rotation frequency and its harmonics. For example, the pressure pulses in internal combustion engines[1] lead to periodic torques, as do the fluctuating torques in electric motors.[2,3] Gear transmission error is another problematic source of noise and vibration in rotating machinery.[4] Resonance in these components can lead to catastrophic failure of the entire machine and even loss of human life. However, if resonances can be detected experimentally then a remedy can be sought, such as increasing or decreasing the mass of certain components, adding torsional dampers, or adjusting operating speeds.

This work is motivated by the need to acquire torsional measurements of either gasoline or diesel engine powered generator sets in the range of 2 to 3000 kW. The alternating displacements of interest range from ±0.00018 to ±4.5 degrees (corresponding to alternating accelerations from ±2120 to ±284,000 deg/s^2), based on various measurements from engines and generators at their nondrive ends. Even smaller motions are expected at the flywheel. These motions are typically dominated by harmonics at whole and half multiples of the engine speed. However, due to such things as cycle to cycle combustion variation and impacts of gear sets, there is typically still some slight excitation at all frequencies. Figure 1 shows a sample torsional measurement from an engine-generator system where the sensor's noise floor was less than the weak signals between

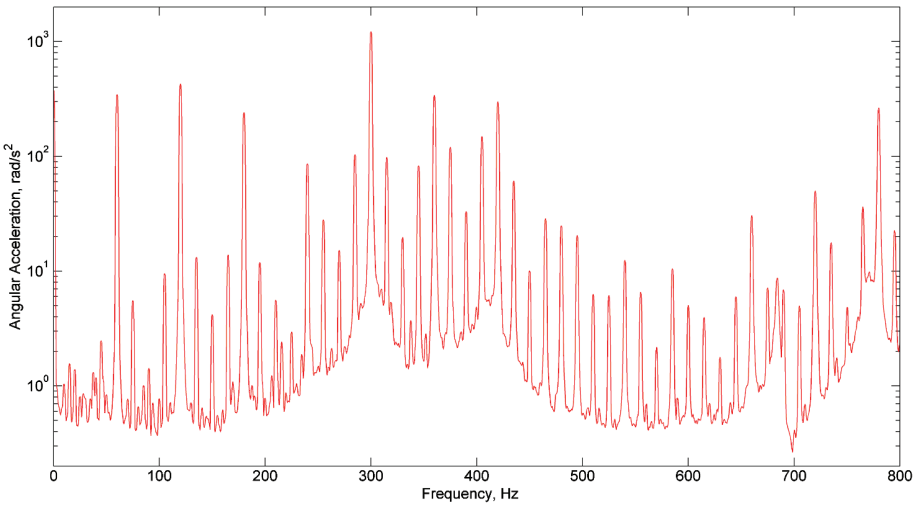

Figure 1 Sample measurement from an electric generator showing the vibration at several harmonics of the rotation frequency and the torsional resonances of the system, which appear as peaks in the noise floor between the dominant harmonics.

engine orders. The response is clearly dominated by motions at whole and half multiples of engine speed, but a weak broadband random response is also visible causing the resonant peaks to be shown in the measurement's noise floor. If the sensor used to acquire the measurement had a noise floor that was one or two orders of magnitude higher, many of those resonances would not have been visible and it would be difficult to identify the modes of the system since the harmonic motions do not clearly reveal the presence of the structure's modes.

Torsional vibrations can be difficult to measure. Any sensor attached to the rotating system cannot be connected to a ground-based data acquisition system without special effort using devices such as slip rings or telemetry. The mass of the sensors and associated hardware must be kept relatively low in order to avoid modifying the structure. In spite of these challenges, torsional accelerometers have recently been developed. Another approach is to use a ground-based sensor to observe the motion of a shaft. For example, the rotational laser vibrometer was recently introduced and shows promise as a noncontact measurement technique. Other devices have also been used to measure angular position and velocity, such as magnetic pickups used to detect the passage of gear teeth, optical pickups with or without special surface treatments,[5] high-resolution rotary encoder systems, and noncontact magnetic sensing encoders. One challenge with many of these systems is that they measure the relative motion between the shaft and the sensor, so care must be taken to assure that the sensor housing is stationary in order to measure its motion accurately.[6]

A few prior works have compared some of the available torsional vibration measurement methods. In Ref. 7, Seidlitz compared a torsional accelerometer with a toothed wheel-magnetic encoder to assess their potential use for measurements from engines. Three generator sets ranging in size from 4 to 1250 kW were considered to span the range of interest. The tests revealed that both instruments were acceptable for the application at hand, but were inaccurate below a particular frequency. The angular accelerometer measurements were found to be inaccurate below 15 Hz, consistent with the minimum sensitivities defined by the manufacturer. The accuracy of the magnetic encoder was found to be dependent on the number of precision teeth used, along with the frequency processing capabilities of the demodulator. In Ref. 8, two methods were presented for reducing spurious order content in encoder type measurements. A correction method was applied to account for nonuniformity in the encoder and found to reduce the spurious order content for less precise encoders. A second algorithm corrected for variation in the shaft speed, reducing the smearing effects from the rotational speed variation for high precision encoders. In Ref. 9, a test was designed to compare the signal from a prototype laser time passage sensor, which was compared to a Hall Effect sensor and glass encoder. The main advantage of the laser was the greater standoff distance allowed. Other works[10] discussed the issues of measurements and processing for incremental geometric encoders, and presented a method for correcting the translational motion of the sensor or rotor.

This work differs from preceding works in two ways. First, a specially designed test rig is used to minimize torsional motion, allowing the noise floor of the sensors to be observed as well as their order content. Second, this work compares a much wider

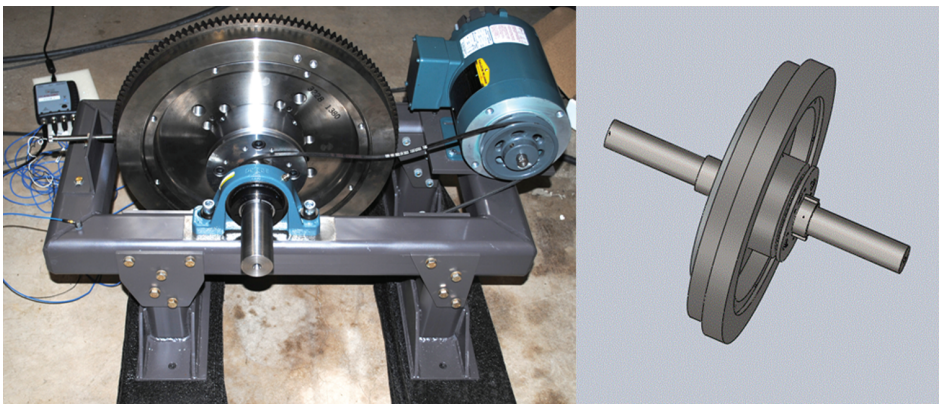

Figure 2 Photograph of torsional vibration test stand (left) and CAD drawing of the flywheel and supporting shaft (right).

range of sensors than any previous study, including accelerometers, encoders of various types, and a laser vibrometer. The following section describes a test rig that was developed in order to compare a large variety of torsional vibration sensors. Measurements were acquired on the test rig from several sensors simultaneously and the performance of each is compared. The results are evaluated revealing the strengths and weaknesses of the sensors.

Experimental Setup

A test stand was designed and manufactured to allow simultaneous measurement from various torsional vibration sensors. The dimensions of the system were chosen to be comparable to those of internal combustion engines that are in common use, to assure relevance to the applications of interest. The goal was to assemble a system that would turn a shaft with minimal angular acceleration so that torsional vibration measurements taken on the rotor would reveal the inherent error, or noise floor, in the sensor. The test rig was designed for rotating speeds between 0 and 1200 rpm with the lowest possible level of angular acceleration, ideally 0.1 rad/s^2 (5.7 deg/s^2) or less. A relatively massive flywheel was coupled rigidly to a stiff rotating shaft, which is driven by a three-phase electric motor (to minimize torque ripple). The motor and flywheel are supported by a steel frame, which was designed such that its first mode of vibration is 10 times greater than the highest driving speed (200 Hz) to reduce the effects of translational motion in the measurement signal. In order to facilitate future works where the test stand will be mounted on a shaker table to evaluate the cross-axis sensitivity of the sensors, the frame and bearings were designed to withstand up to 10 g of vertical acceleration.

Figure 2 shows a photograph of the test stand as well as a schematic of the flywheel and supporting shaft. The frame is constructed of welded A500 steel structural square tube. The frame is approximately 10 inches (25.4 cm) high, 29 inches (73.7 cm) wide, and 14 inches (35.6 cm) deep. The steel drive shaft has a diameter of 1.75 inches (4.45 cm) and is 20 inches (50.8 cm) in length. A massive flywheel (42.4 cm diameter and mass moment of inertia of 1.07 kg $\times$ m^2) mounts to the shaft and is connected with two square steel keys, secured by two set screws. The shaft is mounted to two pillow block bearings which are carefully aligned and bolted to the frame. A three-phase AC motor drives the flywheel shaft and is attached to the frame, as shown in Fig. 2. The motor drives the rotor with a soft, light duty 2L V-belt in order to reduce any torsional oscillations generated by the electric motor. Pulley alignment is critical to prevent unwanted torques applied to the flywheel shaft.

The system was designed so that large diameter encoders could be attached on either end of the flywheel shaft, as well as any sensor (such as the angular accelerometers) that can be bolted to the end of the shaft. The flywheel shaft assembly has 1.75 inch (4.45 cm), 2.25 inch (5.72 cm), 6.0 inch (15.2 cm), 12.0 inch (30.5 cm), and 16.7 inch (42.4 cm) sections so that a torsional laser vibrometer can be applied at various diameters. A ring gear with 138 teeth is also installed on the flywheel so a gear tooth sensor (see far left in Fig. 2) can be used to measure the torsional motion of the flywheel. The drive shaft is long enough to accommodate multiple sensor attachments (e.g. optical sensors, encoders). The following section describes the methodology that was used to minimize torsional vibration of the flywheel shaft, and a description of the measurement systems considered in this work.

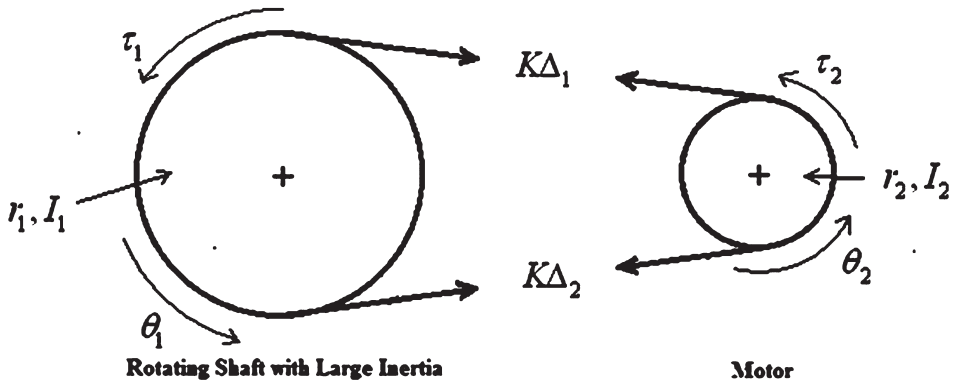

Figure 3 Schematic of 2-DOF model used to design isolation system.

Design of test stand to minimize torsional vibration

No electric motor produces a torque that is perfectly uniform over a revolution of the motor shaft. Motor manufacturers do not typically publish information regarding torque ripple, which is a measure of the observed minimum and maximum output torque over one revolution. This is known to be greater than 100% for some AC motor designs.[11] A three-phase AC motor was chosen in this work, since this class of motor theoretically produces a uniform torque. Even then, the belt drive system was designed to be as soft as possible to isolate the flywheel from any torque oscillations produced by the motor.

A simple design model was used to determine the required belt stiffness to isolate the flywheel from fluctuations in the motor torque. The flywheel–belt-motor system was modeled analytically as a two degree of freedom system, as shown in Fig. 3. This is appropriate if the mass of the belt is much less than the mass of the flywheel and motor, and if the modes of vibration of the motor and flywheel are much greater than the frequency band of interest. The parameters of the system are I_1 and I_2, the mass moment of inertia of the flywheel and motor pulley, respectively, r_1 and r_2 the effective radii of the flywheel and motor pulley, θ_1 and θ_2 their respective angles, and K the stiffness of the belt. The disturbance torques τ_1 and τ_2 are also shown. Dissipation in the belt can also be included with a viscous damping parameter, C. The equation of motion for the flywheel is readily determined using Newton's laws, and can be written as follows:

$$I_1\ddot{\theta}_1 + C\dot{\theta}_1 + 2Kr_1^2\theta_1 = \tau_1 + 2Kr_1r_2\theta_2 \qquad (1)$$

Considering fluctuations in the motor as a disturbance to the system, the natural frequency is $\omega_n = \sqrt{2Kr_1^2/I_1}$, and isolation is achieved at frequencies, ω, much greater than the natural frequency. The frequency response function becomes

$$\theta_1^{\text{accel}}(\omega) \approx \left(\frac{\omega_n}{\omega}\right)^2 \left(\frac{r_2}{r_1}\right) \theta_2^{\text{accel}}(\omega) + \left(\frac{1}{I_1}\right) \tau_1(\omega) \qquad (2)$$

where $\theta_1^{\text{accel}}(\omega)$ denotes the amplitude of the steady-state acceleration of the flywheel.

This reveals that the effect of torques, τ_1, that are applied directly to the flywheel (e.g. due to the bearings or aerodynamic forces) can be minimized by choosing the flywheel inertia to be high. The system can be isolated from the motor torque by choosing the belt stiffness to be low such that the ratio $(\omega_n/\omega)^2$ provides the desired level of isolation. The angular acceleration of a representative motor was measured and found to be on the order of 50 rad/s^2 (2865 deg/s^2), so to provide the desired isolation at 600 rpm (10 Hz), the natural frequency was chosen to be 0.63 Hz with a corresponding belt stiffness 1460 N/m.

The flywheel weighs approximately 41.7 kg with a mass moment of inertia of 1.07 kg m^2, and was dynamically balanced in order to reduce torsional motions of the flywheel shaft. The frictional torque in the bearings should be minimized, as explained by Eq. 2. The bearings were expected to produce an average torque of 0.120 N m at 1200 rpm, based on the product specifications and loading conditions. The manufacturers do not specify the fluctuations in this torque, so for design purposes the bearings were assumed to produce torque fluctuations of this same order. After the test stand was constructed, a coast down test was performed in order to estimate the actual friction torque acting on the flywheel shaft. The motor belt was removed during this test to eliminate its effect on the flywheel motion. The shape of the system's angular velocity as a function of time revealed that the system experiences coulomb,

viscous, and aerodynamic friction during operation. Denoting the corresponding coefficients μ, c, and c_a, respectively, the following equation of motion can be used to model the angular deceleration of the shaft during coast down.

$$I_1\dot{\omega}_1 + c\omega_1 + c_a\omega_1^2 = -\mu N r_b \quad (3)$$

This equation was integrated and each of the parameters (μ, c, and c_a) were manually adjusted until the simulated response visually agreed well with the coast down measurements. Assuming the normal force in the bearings to be $N = 640$ Newtons and the radius at which the coulomb friction force applied is $r_b = 2.54$ cm, the parameters were found to be $\mu = 0.020$, $c = 6.7{\cdot}10^{-3}$ N m s, and $c_a = {\cdot}10^{-6}$ N m s^2. Using these parameters, the frictional loss when running at 600 and 1200 rpm is expected to be 0.75 N m and 1.17 N m, respectively. These values exceed the expected losses in the bearings by an order of magnitude. Hence, the test stand is expected to exhibit angular accelerations up to the order of approximately 1 rad/s^2 (57 deg/s^2). Although this value exceeds the design target, the designed rotor still does exhibit very low angular acceleration.

After the system was manufactured, a modal test was also performed to estimate the modes of the frame/flywheel assembly. The frame was tested in free–free conditions and the results were correlated to an approximate finite element model. The first bending mode of the free–free frame was found to be 196 Hz. The bracket that holds the magnetic pickup sensor (see Fig. 2) was also tested and its first elastic mode was found to be 484 Hz. The correlated finite element model was used to estimate the natural frequencies assuming that the test frame would have been mounted on a rigid base. The fixed base model was predicted to have a first natural frequency of 195 Hz with the shape corresponding to torsional motion of the frame. During all of the noise floor measurement tests described in this work, the frame was bolted to a 36,000 lb (16,330 kg) seismic mass.

Torsional vibration sensors considered

This section lists all of the torsional vibration sensors that were considered in this work, briefly discusses their theory of operation, and provides some details regarding how they were attached to the flywheel system during the tests.

Torsional laser vibrometer

A torsional laser vibrometer is a noncontact sensor that measures the torsional vibration of a rotating object of theoretically arbitrary cross section. A laser of known wavelength is split into two parallel beams of equal intensity and directed at the surface of the rotating object. Both beams of light undergo different Doppler shifts depending on the point at which they are situated and the motion of the object. The beams are mixed and the frequency shift of the mixed beam is measured, providing an estimate for the rotational motion of the test article[12,13] that is theoretically independent of the cross section of the shaft. However, recent work has shown that when speckle noise is present in the vibrometer measurements, the signal noise is certainly affected by the cross section of the shaft (e.g. out of roundness) as well as translational motion of the shaft.[14,15] Since the surfaces at which each laser beam is directed are generally not perpendicular to the laser, retro-reflective tape is typically used to assure that adequate light returns to the photo detector.

The laser vibrometer used in this work was a Polytec® RLV500 with an RLV5000 decoder. This laser has two beams with an offset $d \approx 20$ mm and was used at its optimal standoff distance of 70 mm for all of the measurements. The surfaces of interest were treated with retro-reflective tape (3M Scotchlite Plus, 680 Series with Control Tac Adhesive, Bracknell, UK) and care was taken to minimize the seam in the tape when applying it to each of the sections.

Angular accelerometer

Two angular accelerometers were considered in this work. They are typically used for higher frequencies, when angular displacements are relatively small. The first was an Endevco 7302M1 angular accelerometer which was powered by a Micro-Measurements 2300 series amplifier. The high sensitivity version of this accelerometer was also used. These accelerometers work by sensing the pressure exerted by a ring of fluid that surrounds the rotation axis, as described in Ref. 16. The device is designed to compensate for temperature changes and has been used in a variety of tests. A photograph of one of the devices used in this work is shown in Fig. 4. Slip rings manufactured by Michigan Scientific, Charlevoix, MI, are used to allow the device to be wired to the fixed data acquisition system, as seen in the photograph.

The second was a Kistler 8838 which houses two linear accelerometers at a known offset. The accelerometer signals are subtracted internally to obtain the torsional acceleration. The setup for this sensor was identical to that shown in Fig. 4.

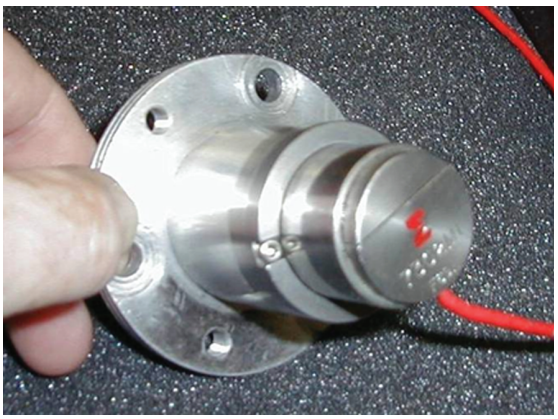

Figure 4 Photograph of an Endevco 7302M1 angular accelerometer with slip rings and the mounting plate that is used to attach it to a rotating shaft or flywheel.

Rotary encoders

Two different rotary encoders were considered in this work. The first was a large diameter Heidenhain ERN 180 with 5000 counts per revolution (CPR). It produces a sinusoidal signal in phase with the passage of the encoder ticks, which is converted to a TTL signal using a Heidenhain IBV600 signal conditioner. The encoder was mounted with a relatively stiff arm to minimize the rotational motion of the housing, but some motion was inevitable so two single-axis translational accelerometers were mounted on the housing to measure the rotational motion of the case. The two accelerometers used were manufactured by PCB Piezotronics, Depew, NY, model number PCB352C16 spaced 104-mm apart on the two sides of the encoder housing.

The second encoder used was a small body Scancon 2RMHF with 1024 CPR. This encoder was allowed to ride freely on the shaft with only the encoder cable providing restraint. Two PCB 352C22 linear accelerometers were mounted on the housing for this encoder, spaced 29.7-mm apart, to capture the rotational motion of the case. The housings of both encoders were observed to move significantly as the shaft rotated. In all of the results presented here, the angular velocity of the case was estimated by taking the difference between the two linear accelerometer measurements and then integrating. The case motion was then subtracted from the encoder signal in order to estimate the true rotational velocity of the shaft.

Magnetic pick-up

A Honeywell variable reluctance sensor (3015A35) was used to measure the passage of teeth on the ring gear to estimate the angular velocity. The passage of a gear tooth near the magnet in the sensor produces a time-varying magnetic flux that induces a proportional voltage in the pickup coil. The voltage signal is processed to calculate the motion of the rotating shaft. The sensor was bolted to a steel bracket with the sensor head mounted very close to the ring gear. The bracket holding the frame was tested and found to have its first bending mode at about 480 Hz, so its rigidity is similar to that of the frame. The ring gear has 138 teeth around its circumference, and is manufactured with a medium precision process (i.e. the gear teeth were not precision ground). This was expected to affect the accuracy of the measurements with the magnetic pick-up sensor.

Optical sensor on zebra tape

An Optel-Thevon 152G7 optical probe was used to measure the passage of 34 equally spaced markings on zebra tape that was adhered to the rotating shaft. The angular velocity was measured by sampling the time duration of the white and black regions of the tape.[5] The sensor was elevated and positioned near the zebra tape with a small tripod such that no motion from the frame was transmitted to the sensor. This setup may not have been optimal; it may have been more effective to mount the sensor to the test frame in order to avoid influence of translation motion on the measurement.

Data collection systems

The signals were captured with three data acquisition systems. The first system was the VISPIRON ROTEC® RAS, which acquired the digital TTL signal with a 10 GHz (40 bit) counter. An absolute time value was saved for each incoming rising flank of the TTL pulse train. Since the 10 GHz clock is common to all channels, numerical round off errors are avoided and accurate cross-channel phasing is obtained. The second system was based on LMS Test.Lab® Signature Testing software and the LMS SCADAS III hardware. The SCADAS III hardware was equipped with a QTV card, which has a 204.8 kHz sample rate to capture the analog signal, from which the zero crossings were estimated. The third system was based on LMS Test.Lab® Signature Testing software and the LMS SCADAS Mobile hardware. The SCADAS Mobile Hardware was equipped with an RV4 module supporting three different pulse train measurement modes. The first mode, named *Analog mode*, used a 204.8 kHz sample rate to capture the signal in analog, from which the zero crossings were estimated. The

second and the third methods acquired the digital TTL signal or the digital RS422/485 signal with a counter running at 820 MHz. The SCADAS RV4 module can measure individual signals or a combination of A, B, and reference signal as typically provided by incremental encoders.

Experimental Results

The test frame was used to acquire measurements from the angular accelerometers, optical encoders, torsional laser, magnetic pickup, and optical sensor with zebra tape. Many of the measurements could be obtained simultaneously because the flywheel shaft had been designed to allow several sensors to be mounted simultaneously. Tests were performed under steady-state rotation at various speeds and during slow startup and coast down, although only steady-state results are presented here. A variety of sensor arrangements were used throughout the test runs to ensure that sufficient data were obtained to make a fair comparison of the noise floor of each sensor. The measurements with the optical encoders and angular accelerometers were expected to offer the lowest noise floor, and hence are used as a baseline when evaluating the rest of the sensors.

Encoders and angular accelerometers

The signals measured by the optical encoders (Heidenhain and Scancon), and the angular accelerometers (Endevco and Kistler) are presented in Fig. 5. The power spectra were processed using a Hanning window and have a resolution of 0.125 Hz. The measurements were acquired as the flywheel ran at a nominally constant speed of 1200 rpm (20 Hz). Since the torsional vibration of the shaft should be nearly zero, the power spectra ideally represented the noise floor of each of the sensors. However, in reality the measurements show several harmonics of the motor rotation frequency, suggesting that the motor causes some speed variation in the flywheel in spite of the efforts made to isolate the two. At those discrete frequencies the inherent vibration in the system dominates the measurement and the noise floor cannot be measured but must be inferred from nearby frequencies.

The measurements show that the performance of each sensor is dependent on the frequency range of interest. At higher frequencies (not shown in Fig. 5), many of the sensors showed a large, broad peak at 1480 Hz, which was believed to be the first torsional mode of the flywheel–shaft assembly. Structural motions of the frame (starting at approximately 200 Hz) do not appear in the spectrum, so the results focus on frequencies up to 1000 Hz. Over most of the frequency range, the high sensitivity Endevco and the Kistler accelerometers (green and red lines) had the best performance, with a noise floor amplitude on the order of $3{\cdot}10^{-8}$ to $1.5{\cdot}10^{-7}$ $(\text{deg/s})^2/\text{Hz}$. The high sensitivity Endevco accelerometer is rated up to 600 Hz, which may explain why its signal degrades at higher frequencies. The standard Endevco sensor is rated up to 1600 Hz, and the Kistler performed well up to 2000 Hz.

Each of the measurements from the optical encoders was corrected by measuring the casing motion and subtracting it from the signal. A discussion of this procedure is provided in the Appendix. The steady-state rotation was measured with the smaller 1024 CPR Scancon encoder using both the LMS RV4 and QTV input modules. The measurements in Fig. 5 show that the baseline noise floor for the RV4 card is lower than that of the QTV (blue and aqua lines), especially at frequencies greater than 200 Hz. Similarly, the 5000 CPR Heidenhain encoder was compared using ROTEC's E-DR input module and LMS's RV4 module (yellow and black lines). In the frequency range of 0 to 1000 Hz, the ROTEC E-DR and LMS RV4 cards offered similar baseline noise floors.

Figure 6 shows the same results that were presented in Fig. 5 over a smaller frequency range between 0 and 120 Hz. At frequencies below 120 Hz, which are of interest to many structural motions, the Endevco angular accelerometers (green and magenta lines) again have the lowest noise floor. The Heidenhain encoder (black and yellow lines) had the next lowest noise floor, independent of the data acquisition system used. The QTV card was not ever used with the Heidenhain encoder because its sample rate was not high enough to accommodate a 5000 CPR encoder at a 1200 rpm rotational speed. The small-body Scancon encoder generally had the highest noise floor of this group of sensors, on the order of 10^{-4} to 10^{-3} $(\text{deg/s})^2/\text{Hz}$. It is also interesting to note that even though the Kistler accelerometer had the lowest noise floor in the 400 to 1,000 Hz range, it performed quite poorly at very low frequencies. This is expected since the Kistler integrates the signal from two piezoelectric accelerometers, and piezoelectric accelerometers typically lose accuracy at low enough frequencies. The high sensitivity Endevco angular accelerometer had the lowest noise floor in this frequency range, as low as 2.7×10^{-8} $(\text{deg/s})^2/\text{Hz}$ at 114 Hz.

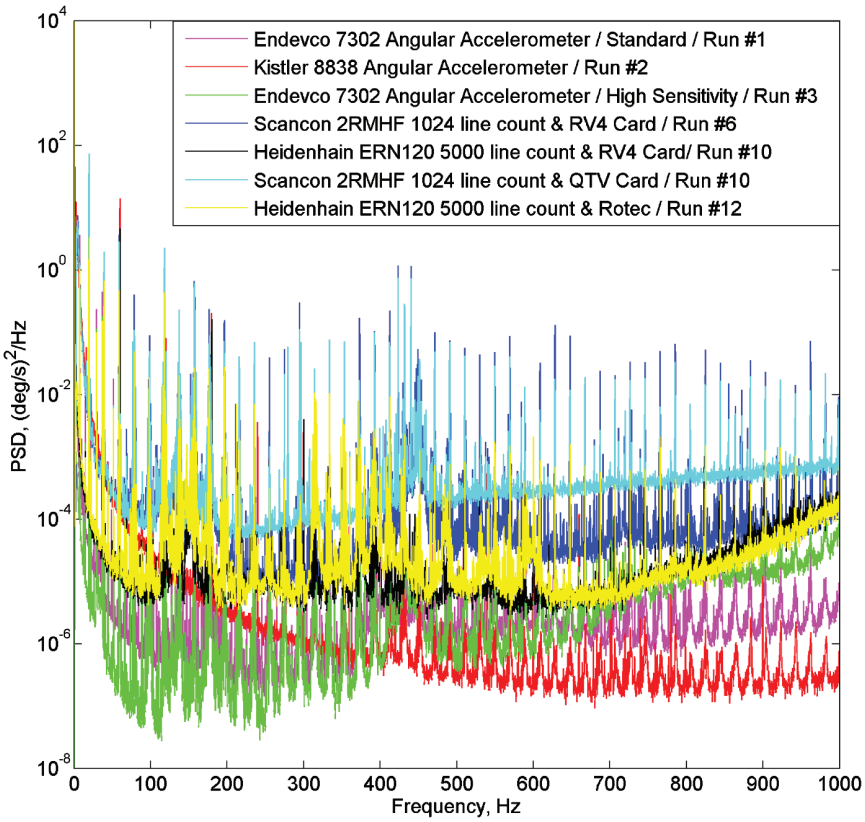

Figure 5 Noise floor comparison of angular accelerometers and encoders between 0 and 1000 Hz, collected at 1200 rpm.

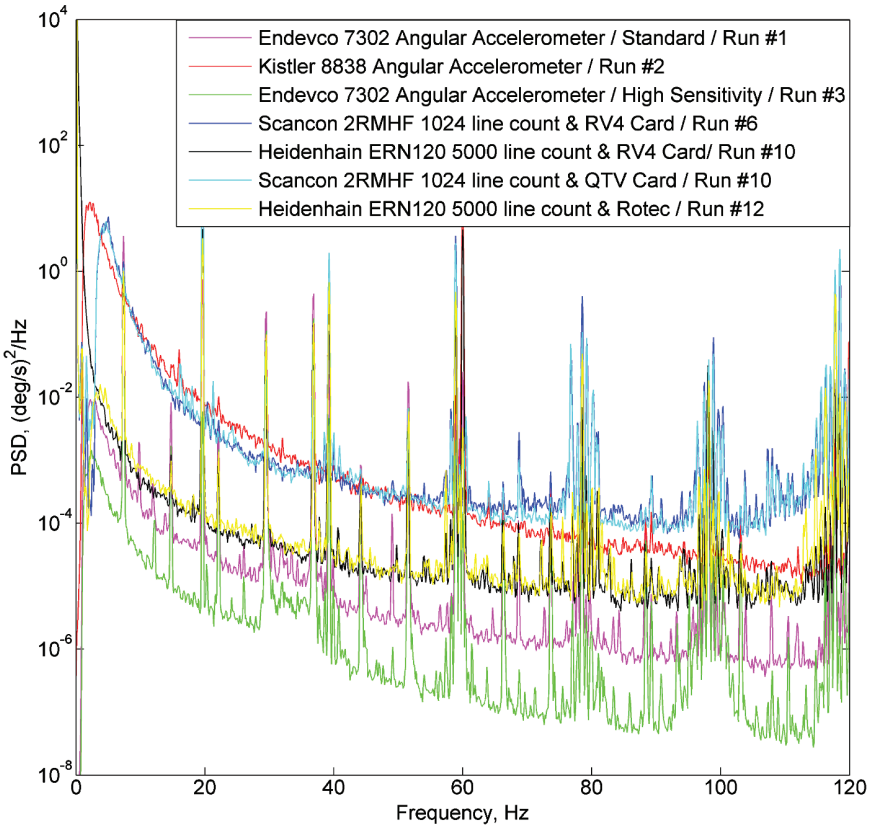

Figure 6 Noise floor comparison of angular accelerometers and encoders between 0 and 120 Hz, collected at 1200 rpm.

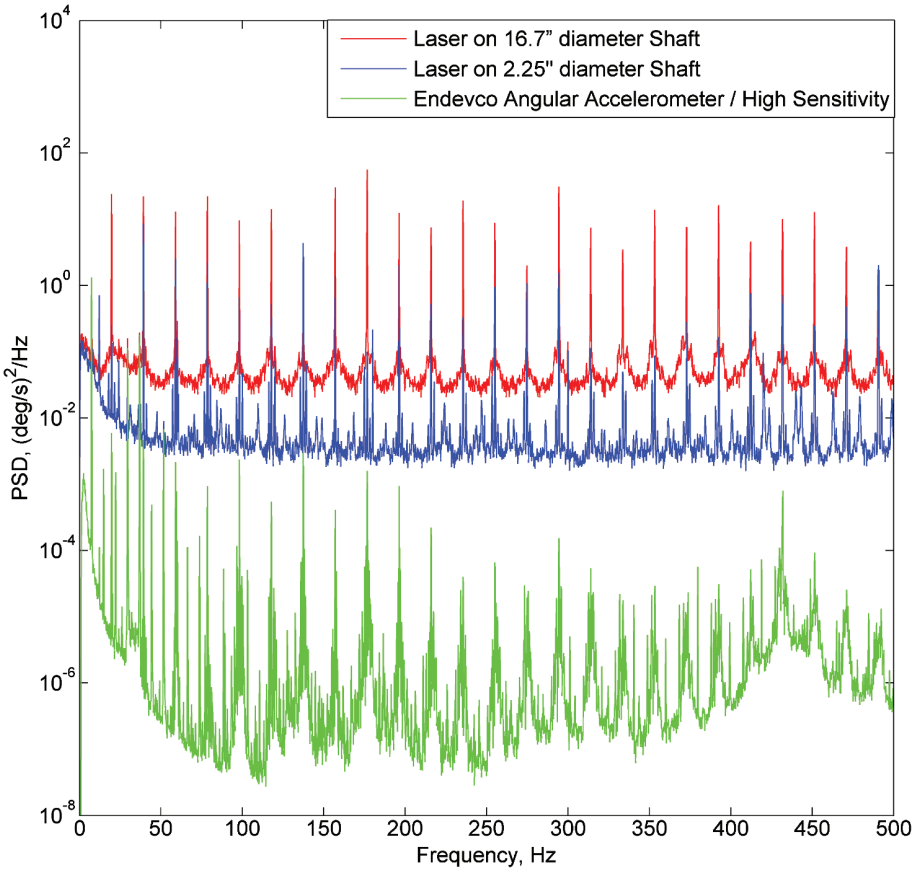

Figure 7 Noise floor comparison of torsional laser and angular accelerometer measurement with laser on shaft diameters of 2.25 inches and 16.7 inches, collected at 1200 rpm.

Torsional laser

The torsional laser acquired measurements during two separate 1200 rpm steady-state tests; one on the 2.25 inch (5.72 cm) diameter of the shaft and the other on the 16.7 inch (42.4 cm) diameter of the flywheel. The torsional laser's noise floor for each shaft diameter is compared in Fig. 7 to that of the high sensitivity Endevco accelerometer, which was one of the best of the sensors in Figs. 5 and 6. The noise floor of the laser was approximately 5 to 6 orders of magnitude higher than the Endevco accelerometer, with little variation between 0 and 500 Hz. At the larger diameter, the noise floor is on the order of 4×10^{-2} $(\text{deg/s})^2/\text{Hz}$ between 0 to 500 Hz, compared to 3×10^{-3} $(\text{deg/s})^2/\text{Hz}$ for the smaller section. On the larger diameter, the rotation caused very little difference between the velocities measured by each of the two lasers, and since the torsion measurement was related to the difference between these velocities, this seemed to increase the noise in the measurement. The sharp peaks in the spectrum from the laser signal all occurred at multiples of the flywheel's rotational speed, and were all probably dominated by laser speckle noise. The speckle noise was approximately periodic because the surface roughness that the laser sees as the flywheel rotates was approximately periodic.[17] At other frequencies only the nonperiodic part of the speckle noise was present, which was at a much lower level. Allen and Sracic noticed similar results when sweeping a similar laser periodically over a surface.[18]

Optical sensor and magnetic pickup on ring gear

Zebra tape was applied to the flywheel shaft so the velocity could be measured with an optical sensor. The setup yielded 34 equidistant black and white stripes per rotation, except for one mark spacing, known as the butt joint, which had a different width than the rest. The butt joint was a result of the application of the tape to the shaft, where the two ends met. This spacing error resulted in a spike in the time history of the velocity signal every time the sensor read the spacing.[5] Here, this anomaly was removed by assuming a value for the angular spacing across the joint and then adjusting that value until the spike in the velocity signal disappeared. The spacing of the remaining pulses was then adjusted to assure that one

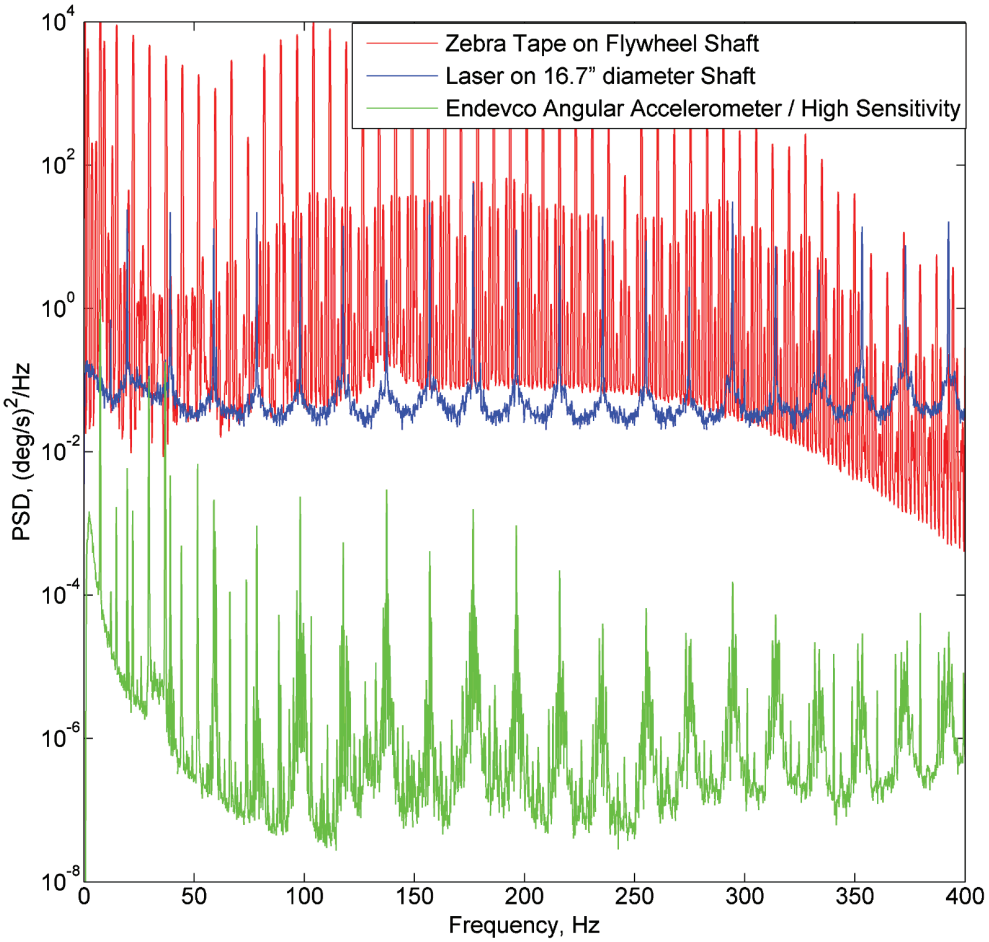

Figure 8 Noise floor comparison of Zebra Tape 34PPR, torsional laser, and angular accelerometer, collected at 1200 rpm.

revolution of the shaft corresponded to 360°, exactly as done in Ref. 5.

Even after applying this correction, the zebra tape still seemed to yield spurious motions at all multiples of rotation speed. Figure 8 compares the noise floor of the optical sensor to the high sensitivity Endevco accelerometer and the torsional laser. At frequencies below 200 Hz, the noise floor of the zebra tape measurement was on the order of 3×10^{-2} to 8×10^{-2} $(\text{deg/s})^2/\text{Hz}$. The performance of the zebra tape measurement was known to depend on the spacing of the black and white stripe pattern attached to the shaft. Only 34 stripes were available in this setup, far fewer than were available to any of the encoders and this was expected to reduce the accuracy of this setup. Figure 9 shows the signal measured by the magnetic pickup sensor on the ring gear with the flywheel shaft rotating at 1050 rpm, compared with the large 5000 CPR Heidenhain encoder. Up to 500 Hz, the noise floor of the magnetic pickup was on the order of 2×10^{-3} $(\text{deg/s})^2/\text{Hz}$, compared to 3×10^{-5} $(\text{deg/s})^2/\text{Hz}$ for the Heidenhain encoder.

Summary of noise floor results

Table 1 compares the minimum noise floors found for each of the sensors and the frequency at which that minimum occurred. As discussed previously, the sensor with the lowest noise floor was the high sensitivity Endevco angular accelerometer, with a noise floor of 2.7×10^{-8} $(\text{deg/s})^2/\text{Hz}$ at 114 Hz. The noise floor for each of the angular accelerometers was on the order of 3×10^{-8} to $2{\cdot}10^{-6}$ $(\text{deg/s})^2/\text{Hz}$, while the optical encoders ranged from 5×10^{-6} to 5×10^{-3} $(\text{deg/s})^2/\text{Hz}$. The noise floor of the torsional laser ranged between 3×10^{-3} and 4×10^{-2} $(\text{deg/s})^2/\text{Hz}$ depending on the diameter of the reflecting shaft. The zebra tape and the magnetic pickup had noise floors ranging from 2×10^{-3} to 8×10^{-2} $(\text{deg/s})^2/\text{Hz}$.

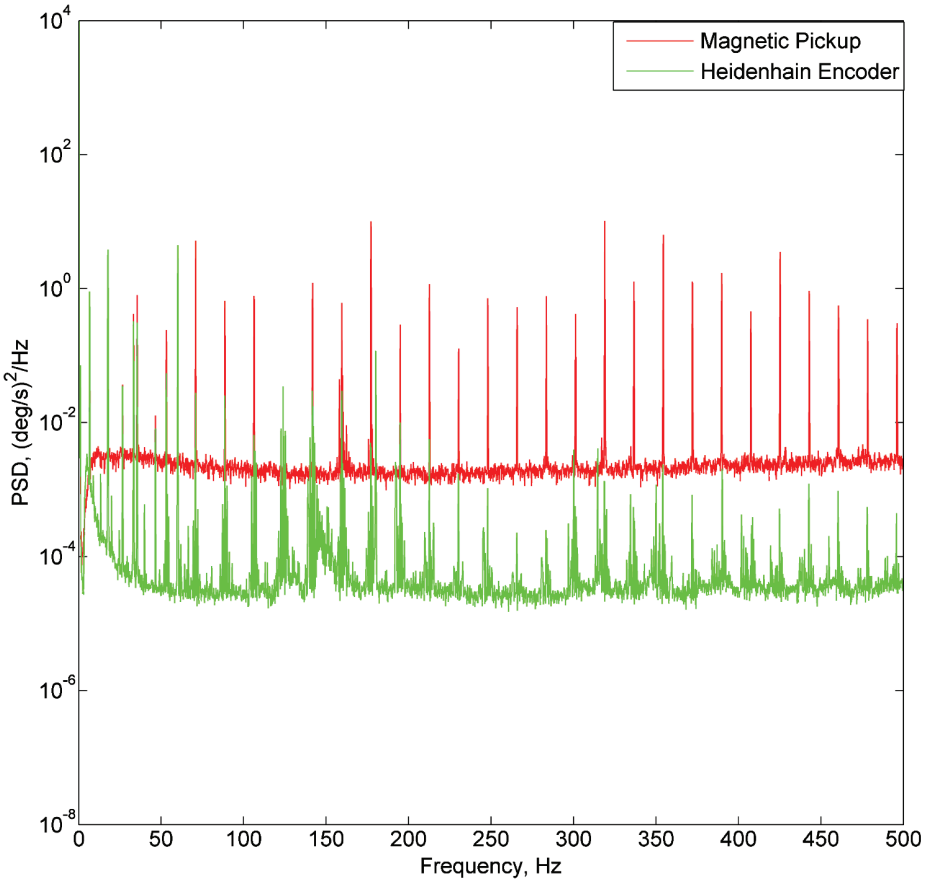

Figure 9 Noise floor comparison of magnetic pickup and encoder, collected at 1050 rpm.

Table 1 Lowest noise floor measurement observed for each of the torsional vibration sensors

	Lowest Noise Floor $[(deg/s)^2/Hz]$	Frequency [Hz]
High sensitivity Endevco Angular Accelerometer	2.7×10^{-8}	114
Kistler Angular Accelerometer	9.2×10^{-8}	681
Standard Endevco Angular Accelerometer	1.4×10^{-7}	249
5000 ppr Heidenhain Encoder with ROTEC System	3.3×10^{-6}	650
5000 ppr Heidenhain Encoder with LMS RV4 Card	2.5×10^{-6}	587
1024 ppr Scancon Encoder with LMS RV4 Card	6.4×10^{-6}	303
1024 ppr Scancon Encoder with LMS QTV Card	4.5×10^{-5}	197
Polytec Torsional Laser on 16.7 inch shaft	2.0×10^{-2}	323
Polytec Torsional Laser on 2.25 inch shaft	1.5×10^{-3}	409
Zebra Tape 34PPR	4.1×10^{-4}	399
Honeywell Variable Reluctance Sensor	9.9×10^{-4}	186

This work is motivated by the need to acquire torsional measurements of either gasoline or diesel engine powered generator sets in the range of 2 to 3000 kW. Figure 10 shows a sample of measured responses from previous tests up to 1000 Hz, where velocity is picked as the common unit. The smallest measured torsional velocity for the range of generator sets is 0.7 deg/s at 540 Hz operating speed. The noise floors of most of the sensors considered would be adequate to capture the torsional vibration of these machines, but only a few of these sensors are capable of capturing low-level vibrations such as those seen in Fig. 1. Of course, the ideal sensor is problem specific since the requirements in other applications may be more or less strict.

Conclusions

A test stand was created and used to compare the noise floor of various torsional vibration sensors. A torsional mode of the flywheel–shaft assembly was discovered near 1480 Hz, limiting the noise floor comparison to below 1000 Hz. No frame motions were observed in any of the torsional vibration measurements within

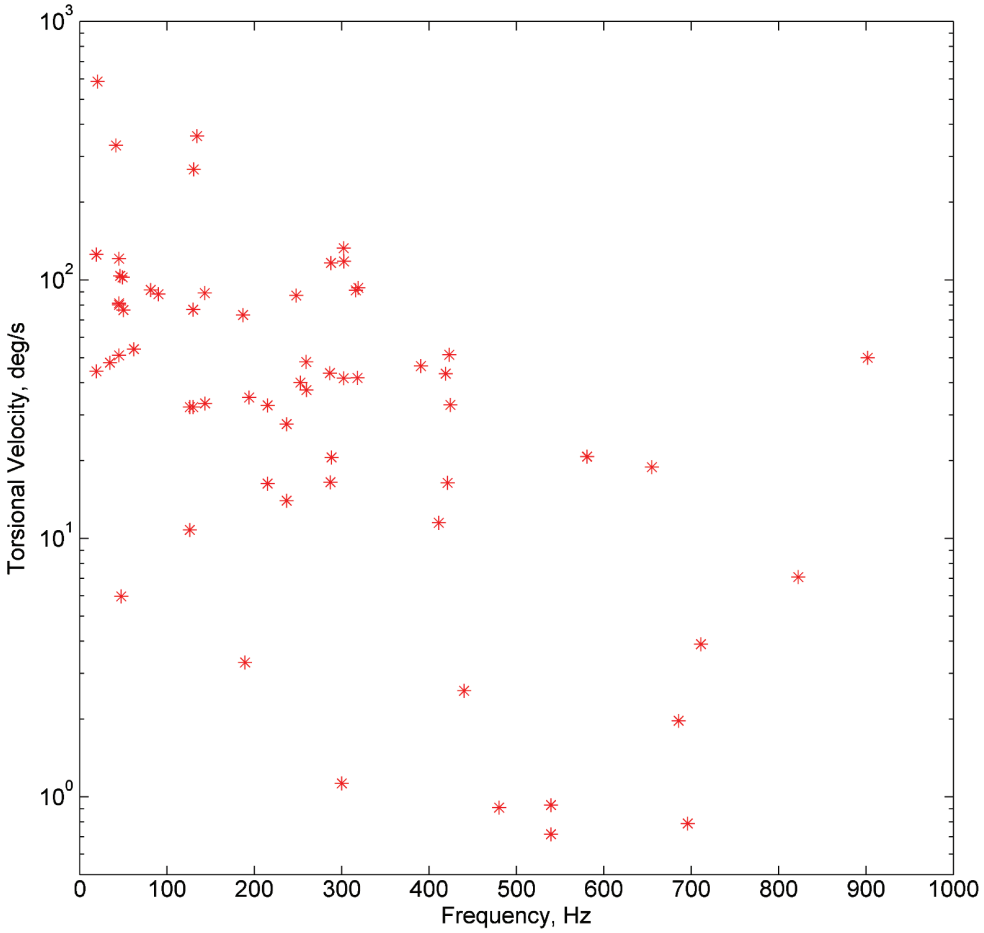

Figure 10 Sample response amplitudes of reciprocating driven generator sets.

this frequency range. The comparison between the angular accelerometers and the optical encoders show that the high sensitivity Endevco produced the lowest noise floor of 2.7×10^{-8} $(\text{deg/s})^2/\text{Hz}$ at 114 Hz. All of the angular accelerometers generally performed well, producing noise floors on the order of 3×10^{-8} to 2×10^{-6} $(\text{deg/s})^2/\text{Hz}$, but their performance degraded below 40 Hz. The encoder based sensors exhibited noise floors ranging from 5×10^{-6} to 5×10^{-3} $(\text{deg/s})^2/\text{Hz}$ over the range of 0 to 1000 Hz. These systems also became less accurate below 40 Hz, apparently because the accelerometers used to correct for the motion of the encoder casings lost accuracy at low frequencies.

The performance of the torsional laser vibrometer was shown to depend strongly on the diameter of the measurement section used. Going from a 16.7-inch (42.4 cm) diameter shaft to a 2.25-inch (5.72 cm) diameter shaft lowered the noise floor by nearly a factor of 10. Selecting a proper shaft diameter could offer better results, but speckle noise is still a concern with the laser vibrometer, and its noise floor was still the highest of all the sensors considered. The magnetic pickup produced a noise floor on the order of 2×10^{-3} $(\text{deg/s})^2/\text{Hz}$. The noise floor for the optical sensor on zebra tape was also found to be quite high, ranging between 2×10^{-3} and 8×10^{-2} $(\text{deg/s})^2/\text{Hz}$. Special care was required with this sensor due to the butt joint in the zebra tape, but a suitable correction was not difficult to apply. A lower noise floor would be expected with a larger shaft diameter allowing more zebra tape stripes per rotation.

Acknowledgments

The authors would like to thank Cummins Power Generation and those involved with the testing. Those individuals include Phil DeBerry from Anger Associates Inc., Laurent Britte, and Bill Flynn from

LMS International, and Doug Hanson, Joe Hauser, and Jason Cheah from Cummins Power Generation.

References

1. Schaberg, P.W., Priede, T., and Dutkiewicz, R.K., "Effects of a Rapid Pressure Rise on Engine Vibration and Noise," *Presented at the SAE International Congress & Exposition*, Detroit, MI, 1990.
2. Ferretti, G., Magnani, G., and Rocco, P., ''Modeling, Identification, and Compensation of Pulsating Torque in Permanent Magnet AC Motors,'' *IEEE Transactions on Industrial Electronics* **45**: 912–920 (1998).
3. Jahns, T.M., and Soong, W.L., ''Pulsating Torque Minimization Techniques for Permanent Magnet AC Motor Drives—A Review,'' *IEEE Transactions on Industrial Electronics* **43**: 321–330 (1996).
4. Sweeney, P.J., and Randall, R.B., ''Gear Transmission Error Measurement Using Phase Demodulation,'' *Proceedings of the Institution of Mechanical Engineers, Part C: Journal of Mechanical Engineering Science* **210**: 201–213 (1996).
5. Janssens, K., Vlierberghe, P.V., D'Hondt, P., Martens, T., Peeters, B., and Claes, W., "Zebra Tape Butt Joint Algorithm for Torsional Vibrations," *Presented at the 28th International Modal Analysis Conference (IMAC XXVIII)*, Jacksonville, FL, 2010.
6. Adamson, S., "Improved Approaches to the Measurement and Analysis of Torsional Vibration," *Presented at the SAE World Congress*, Detroit, MI, 2004.
7. Seidlitz, S., "Engine Torsional Transducer Comparison," *Presented at the SAE International Congress & Exposition*, Detroit, MI, 1992.
8. Resor, B.R., Trethewey, M.W., and Maynard, K.P., ''Compensation for Encoder Geometry and Shaft Speed Variation in Time Interval Torsional Vibration Measurement,'' *Journal of Sound and Vibration* **286**: 897–920 (2005).
9. Trethewey, M.W., Lebold, M.S., and Turner, M.W., "Minimally Intrusive Torsional Vibration Sensing on Rotating Shafts," *Presented at the 28th International Modal Analysis Conference (IMAC XXVIII)*, Jacksonville, FL, 2010.
10. Trethewey, M.W., and Lebold, M.S., "Identification of Torsional Vibration Features in Electrical Powered Rotating Equipment," *Presented at the 27th International Modal Analysis Conference (IMAC XXVII)*, Orlando, FL, 2009.
11. Alger, P.L., *Induction Machines, Their Behavior and Uses*, *Gordon and Breach*, New York (1970).
12. Halliwell, N.A., ''The Laser Torsional Vibrometer: A Step Forward in Rotating Machinery Diagnostics,'' *Journal of Sound and Vibration* **190**: 399–418 (1996).
13. Halliwell, N.A., Pickering, C.J.D., and Eastwood, P.G., ''The Laser Torsional Vibrometer: A New Instrument,'' *Journal of Sound and Vibration* **93**: 588–592 (1984).
14. Martin, P., and Rothberg, S., ''Introducing Speckle Noise Maps for Laser Vibrometry,'' *Optics and Lasers in Engineering* **47**: 431–442 (2009).
15. Martin, P., and Rothberg, S.J., "Differential Measurements Using Two Laser Rotational Vibrometers: Dynamic Backlash," *Presented at the Seventh International Conference on Vibration Measurements by Laser Techniques: Advances and Applications*, Ancona, Italy, 2006.
16. Henry, M.S., "Torsional Vibration Measurement and Analysis: A New Technique," *Presented at the SAE International Off-Highway Meeting & Exposition*, Milwaukee, WI, 1983.
17. Martin, P., and Rothberg, S., ''Introducing Speckle Noise Maps for Laser Vibrometry,'' *Optics and Lasers in Engineering* **47**: 431–442 (2009).
18. Sracic, M.W., and Allen, M.S., "Experimental Investigation of the Effect of Speckle Noise on Continuous Scan Laser Doppler Vibrometer Measurements," *Presented at the 27th International Modal Analysis Conference (IMAC XXVII)*, Orlando, FL, 2009.
19. Rothberg, S., Baker, J., and Halliwell, N.A., ''Laser Vibrometry: Pseudo-Vibrations,'' *Journal of Sound and Vibration* **135**: 516–522 (1989).

Appendix: Encoder Casing Rotation

One issue with an encoder-based measurement system is that it is unable to distinguish between shaft rotation and casing motion. This is a challenge because it is difficult to construct a stiff mount for the encoder that still allows the encoder to move due to any slight eccentricity of the rotating shaft. If the casing motion is not negligible, then it must be measured to correct the encoder signal. The encoder casing rotation was measured by attaching two linear accelerometers to the exterior of the encoder housing. The casing rotation was then computed, integrated and subtracted from the velocity signal measured by the encoder. Figure A1 shows a plot of the time history of the motion of each encoder during steady-state operation at 1200 rpm. The torsional vibration amplitude of the smaller Scancon encoder was approximately 60 deg/s (green line), while the larger Heidenhain encoder had a magnitude of 5 deg/s (red line). As noted previously, the smaller encoder was only restrained by its cable, while the larger encoder was attached to a relatively stiff arm to reduce rotational motion. The Heidenhain encoder casing also has a larger inertia, which may further reduce its rotational motion.

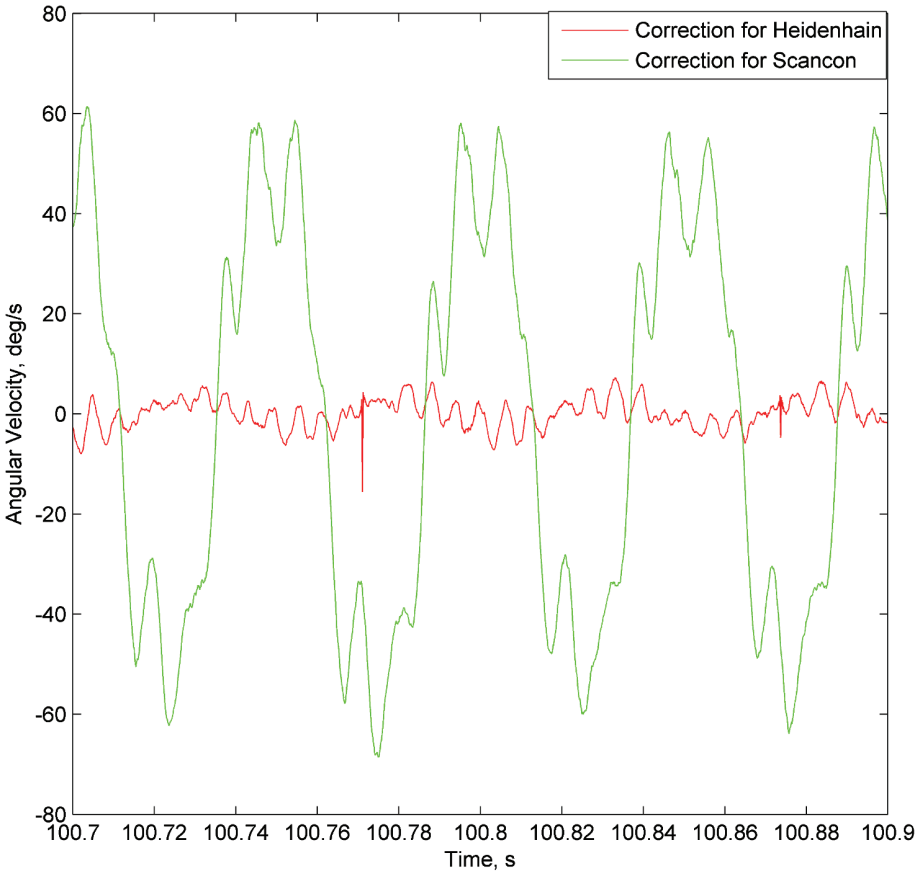

Figure A1 Time history of angular velocity measurement of small and large encoder casings.

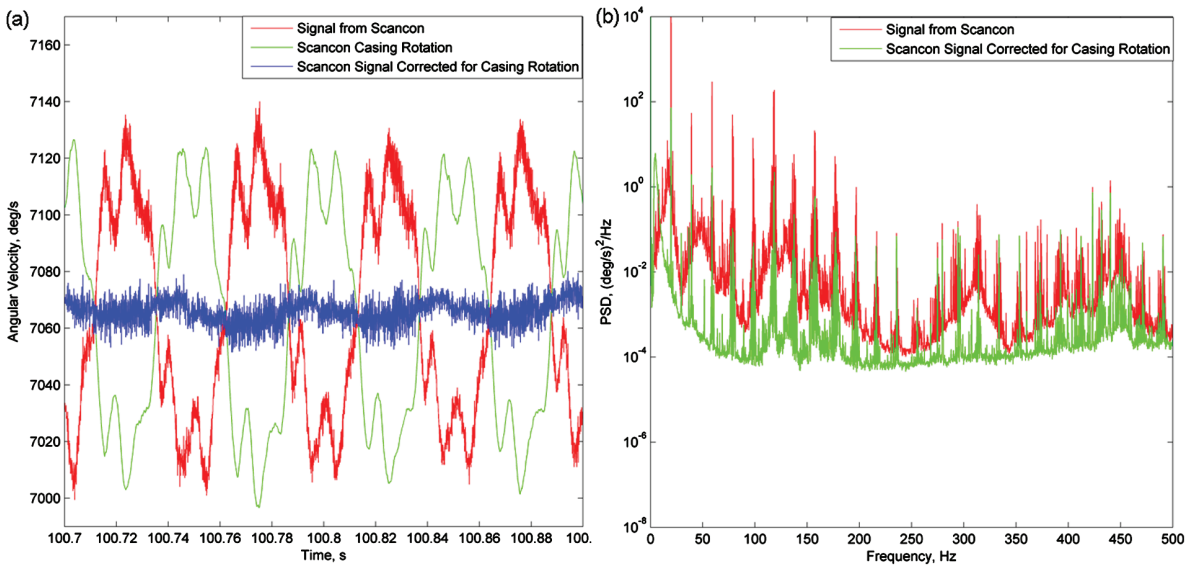

Figure A2 Angular velocity measurements from the small Scancon Encoder. (a) Measured time-domain signals of (red) angular velocity measured by encoder, (green) case motion measured by accelerometers, and (blue) encoder signal after correcting for case motion. (b) Power spectrum of signals of (red) measured encoder signal, and (green) encoder signal after correcting for case motion.

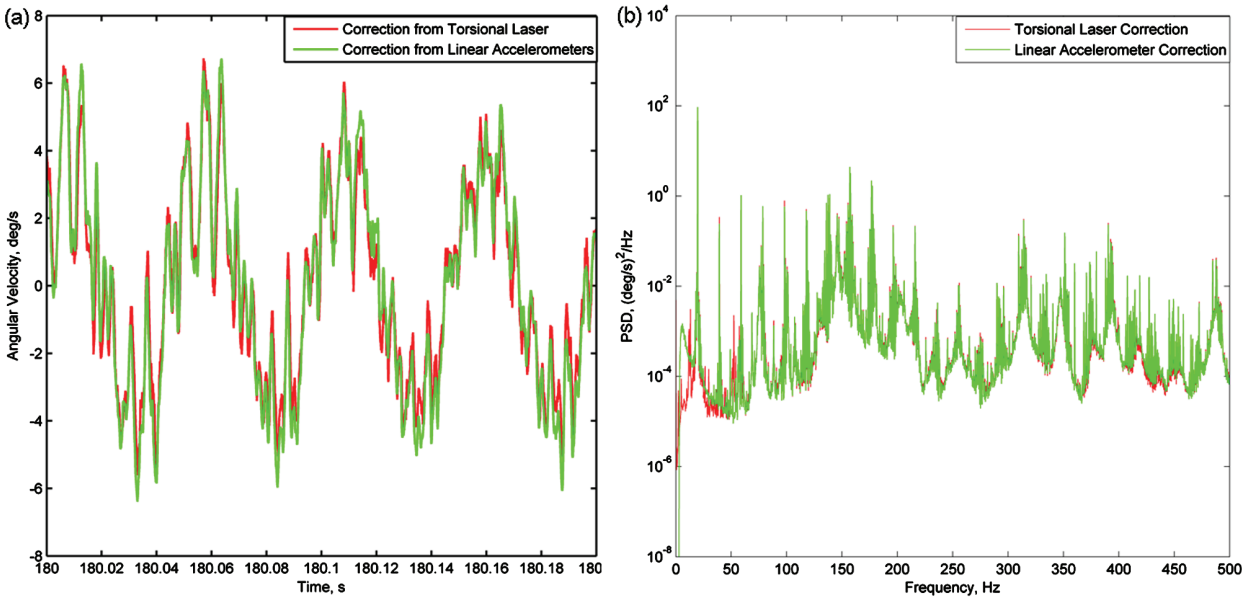

Figure A3 Comparison of casing velocity measured by the torsional laser, compared with the velocity computed using two linear accelerometer measurements in the (a) time and (b) frequency domain. These signals were used to correct the encoder measurements for the casing motion.

The signal from the Scancon casing was collected using two PCB 352C22 accelerometers. These accelerometers are very small and light, and had limited sensitivity at low frequencies. For example, the time history of the rotational velocity of the case is plotted in Fig. A2 (the measured acceleration signals were subtracted to obtain angular acceleration and then integrated to obtain velocity). The encoder signals are also shown, both the measured encoder signal and the corrected encoder signal, which should give the absolute angular velocity of the shaft. The signals show that the encoder signal was dominated by the case motion. After it was subtracted the resulting angular velocity measurement was nearly constant (although somewhat noisy).

The motion of the housing of the large encoder was measured using two methods. First, two linear accelerometers were used, as described above for the smaller encoder, although the Heidenhain encoder was large enough to accommodate two more sensitive, PCB 352C16, accelerometers. For comparison, the Polytec torsional laser was also used to measure the encoder rotation. Figure A3 compares the angular velocity signals obtained from each of these methods. Both methods seem to provide similar corrections to the encoder measurement, although there are some differences below 50 Hz, where one would expect the sensitivity of the accelerometers to degrade. Larger accelerometers with improved sensitivities at low frequencies could have been used to improve the results, since mass loading from the accelerometers was not a concern, and may actually even be preferred since it would increase the inertia of the housing and reduce its motion. On the other hand, if the laser was used one must accept the occasional spikes that occur in the time domain signal due to laser dropout.[19]